MULTIPLE SPACECRAFT FORMATION CONTROL USING $\theta - D$ METHOD

Ming Xin[1], S.N. Balakrishnan[2], H. J. Pernicka[3]

[1,2,3] *Department of Mechanical & Aerospace Engineering, University of Missouri-Rolla*
Rolla, MO 65401, USA

Abstract**:** Multiple spacecraft formation control about the L_2 libration point is investigated in this paper. The circular restricted three-body problem with Sun and Earth as the two primaries is utilized as a framework of study. The idea of virtual structure is considered as the architecture of multiple spacecraft formation. The center of the virtual rigid body follows a nominal orbit around the L_2 libration point. The individual spacecraft is controlled so as to keep a constant relative distance from the center of the virtual structure. A nonlinear model is developed that describes the relative formation dynamics. This nonlinear control problem was addressed by employing a relatively new nonlinear control approach, called the θ-D technique. This method is based on a series solution to the Hamilton_Jacobi_Bellman equation and gives a closed-form suboptimal feedback solution. Simulation results demonstrate that this controller is able to provide millimeter-level formation flying accuracy.

Keywords: Formation Control, Libration Point, Optimal Control, Nonlinear Systems

1. INTRODUCTION

Spacecraft formation flying has been identified by NASA and the U.S. Air Force as a key technology for future deep-space missions. Formation flying is a concept that a group of satellites fly in formation to function as one whole system. It can offer many advantages for which using single spacecraft are difficult to achieve (Leitner, et al., 2001). The development of a reliable, autonomous, and highly accurate formation keeping strategy is required to deploy multiple spacecraft for space missions such as a high accuracy large space interferometer or a large synthetic aperture radar in which a single satellite is not able to realize.

These deep-space missions with high resolution and precision requirements necessitate that a new formation control strategy be developed. There have been a number of studies dealing with formation flying control in the past. Most designs adopt simplifying modeling assumptions such as local linearization about some reference trajectory (Kapila, et al., 2000). However, the simplified linear control strategy may not meet the future deep-space missions' stringent relative position accuracies. A few studies involving nonlinear control of formation flying were investigated in the past: Queiroz et al. (2000) developed an adaptive nonlinear control law based on the full nonlinear dynamics using Lyapunov control design and stability analysis. Gurfil et al. (2003) employed a novel neural adaptive controller to address the deep-space spacecraft formation flying. The controller incorporated an approximate dynamic model inversion, LQR for the ideal feedback linearized model and an adaptive neural-network controller to compensate the model inversion errors. This method demonstrated excellent tracking and achieved submillimeter formation accuracy.

In this paper, we propose a new method, the $\theta - D$ technique (Xin and Balakrishnan, 2005), to design a deep-space formation flying strategy based upon optimal control theory. This strategy uses nonlinear equations of motion of spacecraft in the scenario of the circular restricted three-body problem (CR3BP) with the Sun and the Earth as the primary gravitational bodies. Four-satellite formation flying is considered using the virtual structure (VS)

[1]: Postdoctoral Research Fellow, xin@umr.edu
[2]: Professor, corresponding author, bala@umr.edu
[3]: Associate Professor, pernicka@umr.edu

architecture (Scharf, et al., 2004). In the VS, the entire formation is treated as a single rigid body. The overall motion of the virtual structure and the constant, specified positions and orientations of spacecraft within it are used to generate reference trajectories for the spacecraft to track by using individual spacecraft controllers. Ren and Beard (2004) demonstrated the potential of the VS approach by employing a decentralized scheme for spacecraft formation flying. In this paper, the center of the VS is assumed to follow a reference Lissajous orbit around the L_2 libration point. The relative nonlinear dynamics between the center of VS and spacecraft are derived and a suboptimal closed-form feedback controller is then designed using the $\theta - D$ technique. Numerical results are presented to demonstrate the effectiveness of this method.

2. PROBLEM STATEMENT

The nonlinear equations of motion characterizing spacecraft dynamics are described here in the restricted three-body problem framework. Figure 1 shows the geometry of the restricted three-body problem used in this study. Denote the inertial frame by $(\hat{\mathbf{X}}, \hat{\mathbf{Y}}, \hat{\mathbf{Z}})$ and the rotating frame by $(\hat{\mathbf{x}}, \hat{\mathbf{y}}, \hat{\mathbf{z}})$. Both frames have their origins at the barycenter of the two-body system. The $\hat{\mathbf{x}}$ unit vector is directed from the larger primary toward the smaller primary. The $\hat{\mathbf{y}}$ unit vector is defined normal to the $\hat{\mathbf{x}}$ vector, within the plane of the primaries' orbit, and along the prograde rotational direction. The $\hat{\mathbf{z}}$ unit vector then completes the right-handed frame and is thus normal to the plane of the primaries' orbit. Mass m_1 represents the larger primary and m_2 represents the smaller primary. The nondimensional equations of motion describing the center of the VS for Circular Restricted Three Body Problem are given by

$$\dot{x}_c = 2\dot{y}_c + x_c - \frac{(1-\mu)(x_c+\mu)}{r_1^3} - \frac{\mu[x_c-(1-\mu)]}{r_2^3} + u_{c_1} \quad (1)$$

$$\ddot{y}_c = -2\dot{x}_c + y_c - \frac{(1-\mu)y_c}{r_1^3} - \frac{\mu y_c}{r_2^3} + u_{c_2} \quad (2)$$

$$\ddot{z}_c = -\frac{(1-\mu)z_c}{r_1^3} - \frac{\mu z_c}{r_2^3} + u_{c_3} \quad (3)$$

where (x_c, y_c, z_c) is position of the center of VS in the rotating frame; μ is the ratio of the smaller primary mass to the sum of the masses of both primaries; r_1 and r_2 are the distances from the larger and smaller primary to the center of VS, respectively; and u_x, u_y and u_z are control inputs.

The distance *R* between the two primaries is defined as the unit of length and time is in units of 1/n, where *n* is the mean motion. For the Sun-Earth system

$R = 1.4959787066 \times 10^8$ km, $n = 1.990986606 \times 10^{-7}$

It is assumed that the center of the VS follows a nominal Lissajous trajectory about the Sun-Earth/Moon L_2 libration point and is shown in Fig. 2 in a three-view orthographic projection. This orbit has approximate amplitudes $A_y \cong 300{,}000$ km and $A_z \cong 200{,}000$ km. The 533 day trajectory was numerically integrated in the CR3BP using the method developed by Howell and Pernicka (1988).

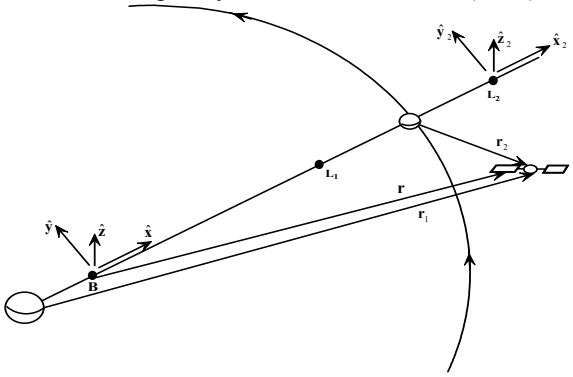

Fig. 1: Basic geometry of the restricted three-body problem

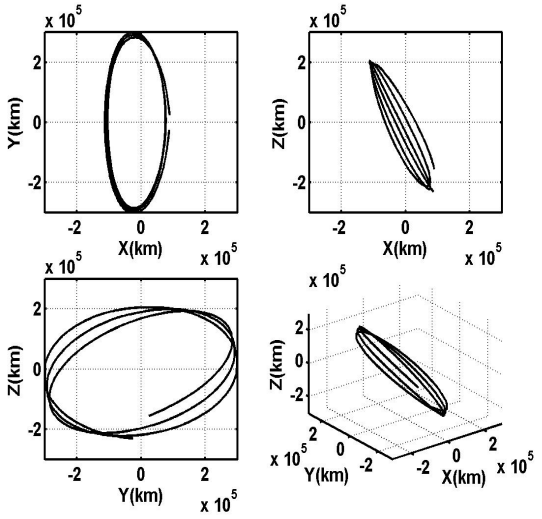

Fig. 2: Nominal Lissajous Orbit about L_2 Libration Point

The relative position vector between the center of the VS and spacecraft can be easily derived as follows (Gurfil et al., 2003):

$$\ddot{x} = 2\dot{y} + x + (1-\mu)\left[\frac{(x_c+\mu)}{r_1^3} - \frac{(x_c+x)+\mu}{\|\boldsymbol{r}_1+\boldsymbol{\rho}\|^3}\right] + \mu\left[\frac{x_c-(1-\mu)}{r_2^3} - \frac{(x_c+x)-(1-\mu)}{\|\boldsymbol{r}_2+\boldsymbol{\rho}\|^3}\right] + u_x \quad (4)$$

$$\ddot{y} = -2\dot{x} + y + (1-\mu)\left[\frac{y_c}{r_1^3} - \frac{y_c+y}{\|\boldsymbol{r}_1+\boldsymbol{\rho}\|^3}\right] + \mu\left[\frac{y_c}{r_2^3} - \frac{y_c+y}{\|\boldsymbol{r}_2+\boldsymbol{\rho}\|^3}\right] + u_y \quad (5)$$

$$\ddot{z} = (1-\mu)\left[\frac{z_c}{r_1^3} - \frac{z_c+z}{\|\boldsymbol{r}_1+\boldsymbol{\rho}\|^3}\right] + \mu\left[\frac{z_c}{r_2^3} - \frac{z_c+z}{\|\boldsymbol{r}_2+\boldsymbol{\rho}\|^3}\right] + u_z \quad (6)$$

where $\boldsymbol{\rho}(x, y, z)$ is the relative position vector between the center of VS and the spacecraft; $u_x = u_{x_s} - u_{x_c}$, $u_y = u_{y_s} - u_{y_c}$, $u_z = u_{z_s} - u_{z_c}$ and u_{x_s}, u_{y_s} and u_{z_s} are control inputs of the spacecraft.

In the next section, a new nonlinear optimal control technique is presented as a formation flying strategy.

3. SUMMARY of $\theta - D$ CONTROL TECHNIQUE

The class of nonlinear time-invariant systems this paper is addressing can be described by

$$\dot{\boldsymbol{x}} = \boldsymbol{f}(\boldsymbol{x}) + \mathbf{g}\boldsymbol{u} \quad (7)$$

with the quadratic cost function:

$$J = \frac{1}{2}\int_0^\infty [\boldsymbol{x}^T\mathbf{Q}\boldsymbol{x} + \boldsymbol{u}^T\mathbf{R}\boldsymbol{u}]dt \quad (8)$$

where $\boldsymbol{x}\in\mathbf{R}^n, \boldsymbol{f}\in\mathbf{R}^n, \mathbf{g}\in\mathbf{R}^{n\times m}, \boldsymbol{u}\in\mathbf{R}^m$, $\mathbf{Q}\in\mathbf{R}^{n\times n}, \mathbf{R}\in\mathbf{R}^{m\times m}$. Assume that $\boldsymbol{x}\in\Omega\subset R^n$ where Ω is a compact set in $\mathbf{R}^n$; $\boldsymbol{f}(\boldsymbol{x})$ is continuously differentiable in $\boldsymbol{x}$ and $\mathbf{g}$ is a constant matrix; The condition $\boldsymbol{f}(\mathbf{0})=\mathbf{0}$ is assumed in order to have the system at equilibrium when it is at the origin. $\mathbf{Q}$ is assumed to be a positive semi-definite constant matrix and $\mathbf{R}$ is assumed to be a positive-definite constant matrix.

The optimal solution of the infinite-horizon nonlinear regulator problem can be obtained by solving the Hamilton-Jacobi-Bellman (HJB) partial differential equation (Bryson and Ho, 1975):

$$\frac{\partial V^T}{\partial \boldsymbol{x}}\mathbf{f}(\boldsymbol{x})-\frac{1}{2}\frac{\partial V^T}{\partial \boldsymbol{x}}\mathbf{g}\mathbf{R}^{-1}\mathbf{g}^T\frac{\partial V}{\partial \boldsymbol{x}}+\frac{1}{2}\boldsymbol{x}^T\mathbf{Q}\boldsymbol{x}=0 \tag{9}$$

where $V(\boldsymbol{x})$ is the optimal cost , i.e.

$$V(\boldsymbol{x})=\min_{\mathbf{u}}\frac{1}{2}\int_0^\infty(\boldsymbol{x}^T\mathbf{Q}\boldsymbol{x}+\boldsymbol{u}^T\mathbf{R}\boldsymbol{u})dt \tag{10}$$

It is assumed that $V(\boldsymbol{x})$ is continuously differentiable and $V(\boldsymbol{x})>0$ with $V(\mathbf{0})=0$.

The necessary condition for optimality leads to

$$\boldsymbol{u}=-\mathbf{R}^{-1}\mathbf{g}^T\frac{\partial V}{\partial \boldsymbol{x}} \tag{11}$$

The HJB equation is very difficult to get the closed-form solution. In this paper, a suboptimal control synthesis technique that will solve the HJB equation approximately is presented.

Now consider perturbations added to the cost function:

$$J=\frac{1}{2}\int_0^\infty[\boldsymbol{x}^T(\mathbf{Q}+\sum_{i=1}^{\infty}\mathbf{D}_i\theta^i)\boldsymbol{x}+\boldsymbol{u}^T\mathbf{R}\boldsymbol{u}]dt \tag{12}$$

These perturbations are used to modulate the system transient response and their computations are discussed later.

Rewrite the original state equation as:

$$\dot{\boldsymbol{x}}=\boldsymbol{f}(\boldsymbol{x})+\mathbf{g}\boldsymbol{u}=\boldsymbol{F}(\boldsymbol{x})\boldsymbol{x}+\mathbf{g}\boldsymbol{u}=\left\{\mathbf{A}_0+\theta\left[\frac{\mathbf{A}(\boldsymbol{x})}{\theta}\right]\right\}\boldsymbol{x}+\mathbf{g}\boldsymbol{u} \tag{13}$$

where θ is an intermediate scalar variable; $\mathbf{A_0}$ is a constant coefficient matrix such that $(\mathbf{A_0},\mathbf{g})$ is a stabilizable pair and $[\mathbf{A_0}+\mathbf{A}(\boldsymbol{x}),\mathbf{g}]$ is pointwise controllable.

Define

$$\boldsymbol{\lambda}=\frac{\partial V}{\partial \boldsymbol{x}} \tag{14}$$

By using (14) in (9) and using the perturbed cost function, the perturbed HJB equation becomes

$$\boldsymbol{\lambda}^T\boldsymbol{f}(\boldsymbol{x})-\frac{1}{2}\boldsymbol{\lambda}^T\mathbf{g}\mathbf{R}^{-1}\mathbf{g}^T\boldsymbol{\lambda}+\frac{1}{2}\boldsymbol{x}^T(\mathbf{Q}+\sum_{i=1}^{\infty}\mathbf{D}_i\theta^i)\boldsymbol{x}=0 \tag{15}$$

Assume a power series expansion of $\boldsymbol{\lambda}$ as

$$\boldsymbol{\lambda}=\sum_{i=0}^{\infty}\mathbf{T}_i\theta^i\boldsymbol{x} \tag{16}$$

where $\mathbf{T}_i$ are to be determined and assumed to be symmetric.

Substitute equation (16) into equation (15) and equate the coefficients of powers of θ to zero to get the following equations:

$$\mathbf{T}_0\mathbf{A}_0+\mathbf{A}_0{}^T\mathbf{T}_0-\mathbf{T}_0\mathbf{g}\mathbf{R}^{-1}\mathbf{g}^T\mathbf{T}_0+\mathbf{Q}=\mathbf{0} \tag{17}$$

$$\mathbf{T}_1(\mathbf{A}_0-\mathbf{g}\mathbf{R}^1\mathbf{g}^T\mathbf{T}_0)+(\mathbf{A}_0^T-\mathbf{T}_0\mathbf{g}\mathbf{R}^{-1}\mathbf{g}^T)\mathbf{T}_1=-\frac{\mathbf{T}_0\mathbf{A}(\boldsymbol{x})}{\theta}-\frac{\mathbf{A}^T(\boldsymbol{x})\mathbf{T}_0}{\theta}-\mathbf{D}_1 \tag{18}$$

$$\vdots$$

$$\mathbf{T}_n(\mathbf{A}_0-\mathbf{g}\mathbf{R}^{-1}\mathbf{g}^T\mathbf{T}_0)+(\mathbf{A}_0^T-\mathbf{T}_0\mathbf{g}\mathbf{R}^{-1}\mathbf{g}^T)\mathbf{T}_n=-\frac{\mathbf{T}_{n-1}\mathbf{A}(\boldsymbol{x})}{\theta}-\frac{\mathbf{A}^T(\boldsymbol{x})\mathbf{T}_{n-1}}{\theta}+\sum_{j=1}^{n-1}\mathbf{T}_j\mathbf{g}\mathbf{R}^{-1}\mathbf{g}^T\mathbf{T}_{n-j}-\mathbf{D}_n \tag{19}$$

Since the right hand side of equations (18)-(19) involve $\boldsymbol{x}$ and θ, $\mathbf{T}_i$ would be the function of $\boldsymbol{x}$ and θ. Thus it is denoted as $\mathbf{T}_i(\boldsymbol{x},\theta)$.

Control can be obtained in terms of the power series for $\boldsymbol{\lambda}$ as

$$\boldsymbol{u}=-\mathbf{R}^{-1}\mathbf{g}^T\boldsymbol{\lambda}=-\mathbf{R}^{-1}\mathbf{g}^T\sum_{i=0}^{\infty}\mathbf{T}_i(\boldsymbol{x},\theta)\theta^i\boldsymbol{x} \tag{20}$$

Construct the following expression for $\mathbf{D}_i$:

$$\mathbf{D}_1=k_1e^{-l_1t}[-\frac{\mathbf{T}_0\mathbf{A}(\boldsymbol{x})}{\theta}-\frac{\mathbf{A}^T(\boldsymbol{x})\mathbf{T}_0}{\theta}] \tag{21}$$

$$\vdots$$

$$\mathbf{D}_n=k_ne^{-l_nt}[-\frac{\mathbf{T}_{n-1}\mathbf{A}(\boldsymbol{x})}{\theta}-\frac{\mathbf{A}^T(\boldsymbol{x})\mathbf{T}_{n-1}}{\theta}+\sum_{j=1}^{n-1}\mathbf{T}_j\mathbf{g}\mathbf{R}^{-1}\mathbf{g}^T\mathbf{T}_{n-j}] \tag{22}$$

where k_i and $l_i>0, i=1,\cdots n$ are adjustable design parameters.

$\mathbf{D}_i$ is chosen such that

$$-\frac{\mathbf{T}_{i-1}\mathbf{A}(\boldsymbol{x})}{\theta}-\frac{\mathbf{A}^T(\boldsymbol{x})\mathbf{T}_{i-1}}{\theta}+\sum_{j=1}^{i-1}\mathbf{T}_j\mathbf{g}\mathbf{R}^{-1}\mathbf{g}^T\mathbf{T}_{i-j}-\mathbf{D}_i=\varepsilon_i(t)\left[-\frac{\mathbf{T}_{i-1}\mathbf{A}(\boldsymbol{x})}{\theta}-\frac{\mathbf{A}^T(\boldsymbol{x})\mathbf{T}_{i-1}}{\theta}+\sum_{j=1}^{i-1}\mathbf{T}_j\mathbf{g}\mathbf{R}^{-1}\mathbf{g}^T\mathbf{T}_{i-j}\right], i=1,\cdots n \tag{23}$$

where $\varepsilon_i(t)=1-k_ie^{-l_it}$ is a small number. $\varepsilon_i(t)$ is chosen to satisfy some conditions required in the proof of convergence and stability of the above algorithm (Xin and Balakrishnan, 2005). On the other hand, the exponential term e^{-l_it} with $l_i>0$ is used to let the perturbation terms in the cost function and HJB equation diminish as time evolves. In addition, $\varepsilon_i(t)$ can be used to suppress the initial large control from happening in equations (17) through (19). k_i and l_i in the $\mathbf{D}_i$ are design parameters which allow flexibility to modulate the system transient performance.

Since Eqs. (18), (19) are linear equations in terms of $\mathbf{T}_2,\cdots,\mathbf{T}_n$ and the coefficient matrices of these equations are constant matrices, closed-form solutions for $\mathbf{T}_2,\cdots,\mathbf{T}_n$ can be obtained with just one matrix inverse operation. The expressions of the right hand side of the equations are already known and needs only simple matrix multiplications and additions.

Remark: θ is just an intermediate variable. The introduction of θ is for the convenience of writing $\boldsymbol{\lambda}$ as a power series expansion. θ turns out to be cancelled when $\mathbf{T}_i(\boldsymbol{x},\theta)$ multiplies θ^i in the final control calculations, i.e. Eq. (20).

As can be seen, the $\theta-D$ controller is a closed-form suboptimal feedback solution to the nonlinear optimal regulator problem if a finite number of terms in control are taken. It can also achieve semi-global asymptotic stability. For detailed proof of stability and convergence of the series $\sum_{i=0}^{\infty}\mathbf{T}_i(\boldsymbol{x},\theta)\theta^i$ the

reader is referred to Xin and Balakrishnan, 2005. Also in this reference, some benchmark nonlinear control problems are investigated to show how close to the optimal control solution the $\theta-D$ method can achieve. The $\theta-D$ method provides a *closed-form* feedback controller for the nonlinear optimal control problem and therefore, is a candidate for real time implementation. In the next section, this new technique is employed to solve the nonlinear formation control problem.

4. FORMATION CONTROL EMPLOYING $\theta-D$ TECHNIQUE

The controller design for each spacecraft in the formation follows the same procedure as described in the last section. Hence, only one spacecraft is considered in the following development. To synthesize the control law, it is convenient to use the state-space representation. To this end, we define the state vector for the center of the VS and the relative state vector between the center of the VS and the spacecraft:

$$\boldsymbol{x}_c \triangleq [x_c \;\; \dot{x}_c \;\; y_c \;\; \dot{y}_c \;\; z_c \;\; \dot{z}_c]^T, \boldsymbol{x}_s \triangleq [x \;\; \dot{x} \;\; y \;\; \dot{y} \;\; z \;\; \dot{z}]^T \quad (24)$$

where $\boldsymbol{x}_c$ and $\boldsymbol{x}_s$ satisfy the dynamic equations (1)-(3) and (4)-(6) respectively. They can be written in a general form:

$$\dot{\boldsymbol{x}}_c = \boldsymbol{f}_c(\boldsymbol{x}_c) + \boldsymbol{u}_c \quad (25)$$

$$\dot{\boldsymbol{x}}_s = \boldsymbol{f}_s(\boldsymbol{x}_s, \boldsymbol{x}_c) + \boldsymbol{u} \quad (26)$$

As seen from Eqs. (25) and (26), the controller design for the center of the VS and the spacecraft can be carried out separately. $\boldsymbol{x}_c$ can be considered as independent variables to the equations of the relative dynamics. An expression for relative control will be developed in this section. The control of the center of the VS follows a similar procedure.

The cost function is chosen to be a quadratic function of the state and control

$$J = \frac{1}{2}\int_0^\infty [\boldsymbol{x}_s^T \mathbf{Q} \boldsymbol{x}_s + \boldsymbol{u}^T \mathbf{R} \boldsymbol{u}] dt \quad (27)$$

The weighting functions are chosen to be:

$$\mathbf{Q} = diag\{q_{11}, q_{22}, q_{33}, q_{44}, q_{55}, q_{66}\}, \; \mathbf{R} = diag\{r_{11}, r_{22}, r_{33}\} \quad (28)$$

In order to employ the $\theta-D$ method, the condition $\boldsymbol{f}(\mathbf{0}) = \mathbf{0}$ has to be satisfied. However, the terms

$$(1-\mu)\left[\frac{(x_c+\mu)}{r_1^3} - \frac{(x_c+\mu)}{\|\boldsymbol{r}_1+\boldsymbol{\rho}\|^3}\right] + \mu\left[\frac{x_c-(1-\mu)}{r_2^3} - \frac{x_c-(1-\mu)}{\|\boldsymbol{r}_2+\boldsymbol{\rho}\|^3}\right]$$

in Eq. (4),

$$(1-\mu)\left[\frac{y_c}{r_1^3} - \frac{y_c}{\|\boldsymbol{r}_1+\boldsymbol{\rho}\|^3}\right] + \mu\left[\frac{y_c}{r_2^3} - \frac{y_c}{\|\boldsymbol{r}_2+\boldsymbol{\rho}\|^3}\right] \text{ in Eq. (5)}$$

and $(1-\mu)\left[\frac{z_c}{r_1^3} - \frac{z_c}{\|\boldsymbol{r}_1+\boldsymbol{\rho}\|^3}\right] + \mu\left[\frac{z_c}{r_2^3} - \frac{z_c}{\|\boldsymbol{r}_2+\boldsymbol{\rho}\|^3}\right]$ in Eq. (6) are bias terms which will not go to zero when the states are zero. Therefore, an additional state 's' with stable dynamics is added to the state space in order to absorb the biases (Xin and Balakrishnan, 2004)

$$\dot{s} = -\lambda_s s \quad (29)$$

Note that this new variable will not alter the basic dynamics since those bias terms are treated by multiplying and dividing them by s. It is reset to its initial value at each integration step in the simulation. The augmented state variable is defined as $\tilde{\boldsymbol{x}}_s = [\boldsymbol{x}_s \quad s]^T$.

To apply the $\theta-D$ control design, it is required to write the original nonlinear equations into a linear-like structure:

$$\dot{\tilde{\boldsymbol{x}}}_s = \boldsymbol{F}(\tilde{\boldsymbol{x}}_s)\tilde{\boldsymbol{x}}_s + \mathbf{g}\boldsymbol{u} \quad (30)$$

where

$$\boldsymbol{F}(\tilde{\boldsymbol{x}}) = \begin{bmatrix} 0 & 1 & 0 & 0 & 0 & 0 & 0 \\ a_{21} & 0 & 0 & 2 & 0 & 0 & a_{27} \\ 0 & 0 & 0 & 1 & 0 & 0 & 0 \\ 0 & -2 & a_{43} & 0 & 0 & 0 & a_{47} \\ 0 & 0 & 0 & 0 & 0 & 1 & 0 \\ 0 & 0 & 0 & 0 & a_{65} & 0 & a_{67} \\ 0 & 0 & 0 & 0 & 0 & 0 & -\lambda_s \end{bmatrix}, \; \mathbf{g} = \begin{bmatrix} 0 & 0 & 0 \\ 1 & 0 & 0 \\ 0 & 0 & 0 \\ 0 & 1 & 0 \\ 0 & 0 & 0 \\ 0 & 0 & 1 \\ 0 & 0 & 0 \end{bmatrix} \quad (31)$$

where

$$a_{21} = 1 - \frac{1-\mu}{\|\boldsymbol{r}_1+\boldsymbol{\rho}\|^3} - \frac{\mu}{\|\boldsymbol{r}_2+\boldsymbol{\rho}\|^3}, \; a_{43} = 1 - \frac{1-\mu}{\|\boldsymbol{r}_1+\boldsymbol{\rho}\|^3} - \frac{\mu}{\|\boldsymbol{r}_2+\boldsymbol{\rho}\|^3}$$

$$a_{27} = (1-\mu)\left[\frac{(x_c+\mu)}{r_1^3 s} - \frac{(x_c+\mu)}{\|\boldsymbol{r}_1+\boldsymbol{\rho}\|^3 s}\right] + \mu\left[\frac{x_c-(1-\mu)}{r_2^3 s} - \frac{x_c-(1-\mu)}{\|\boldsymbol{r}_2+\boldsymbol{\rho}\|^3 s}\right],$$

$$a_{47} = (1-\mu)\left[\frac{y_c}{r_1^3 s} - \frac{y_c}{\|\boldsymbol{r}_1+\boldsymbol{\rho}\|^3 s}\right] + \mu\left[\frac{y_c}{r_2^3 s} - \frac{y_c}{\|\boldsymbol{r}_2+\boldsymbol{\rho}\|^3 s}\right]$$

$$a_{65} = -\frac{(1-\mu)}{\|\boldsymbol{r}_1+\boldsymbol{\rho}\|^3} - \frac{\mu}{\|\boldsymbol{r}_2+\boldsymbol{\rho}\|^3},$$

$$a_{67} = (1-\mu)\left[\frac{z_c}{r_1^3 s} - \frac{z_c}{\|\boldsymbol{r}_1+\boldsymbol{\rho}\|^3 s}\right] + \mu\left[\frac{z_c}{r_2^3 s} - \frac{z_c}{\|\boldsymbol{r}_2+\boldsymbol{\rho}\|^3 s}\right]$$

In the $\theta-D$ formulation, the factorization of the nonlinear equation (13) is chosen to be:

$$\dot{\tilde{\boldsymbol{x}}}_s = \left[\boldsymbol{F}(\tilde{\boldsymbol{x}}_s(t_0)) + \theta\left(\frac{\boldsymbol{F}(\tilde{\boldsymbol{x}}_s) - \boldsymbol{F}(\tilde{\boldsymbol{x}}_s(t_0))}{\theta}\right)\right]\tilde{\boldsymbol{x}}_s + \boldsymbol{g}\boldsymbol{u} \quad (32)$$

The advantage of choosing this factorization is that in the $\theta-D$ formulation $\mathbf{T}_0$ is solved from $\mathbf{A}_0$ and $\mathbf{g}$ in (17) and $\mathbf{T}_0$ would have a good starting point if $\mathbf{A}_0$ is chosen to be $\mathbf{A}_0 = \boldsymbol{F}(\tilde{\boldsymbol{x}}_s(t_0))$ since $\mathbf{A}(\tilde{\boldsymbol{x}}_s(t_0))$ retains much more system information than an arbitrary choice of $\mathbf{A}_0$ would.

The final feedback controller takes the form of

$$\boldsymbol{u} = -\mathbf{R}^{-1}\mathbf{g}^T\left[\mathbf{T}_0 + \mathbf{T}_1(\tilde{\boldsymbol{x}}_s, \theta)\theta + \mathbf{T}_2(\tilde{\boldsymbol{x}}_s, \theta)\theta^2\right](\tilde{\boldsymbol{x}}_s - \tilde{\boldsymbol{x}}_r) \quad (33)$$

where $\tilde{\boldsymbol{x}}_r = [x_r \;\; \dot{x}_r \;\; y_r \;\; \dot{y}_r \;\; z_r \;\; \dot{z}_r \;\; 0]^T$ is the reference relative trajectory. This trajectory could be a predefined time-varying relative trajectory or simply a constant offset.

5. NUMERICAL RESULTS AND ANALYSIS

Problem of keeping a constellation of four spacecraft in a square formation in the rotational frame is considered in this paper. This can be easily generalized to any formation in an inertial frame. A square formation is arbitrarily selected to demonstrate the control technique. As a benchmark formation flying study, the required formation accuracy is less than 1 centimeter. The center of the VS follows the nominal Lissajous trajectory about

the L_2 libration point which is shown in Fig. 2. The initial conditions of the center of the VS reference trajectory computed in Section 2 are given by

$x_0 = 87028.508409273$ km, $y_0 = -24739.512629980$ km,

$z_0 = -229951.974656271$ km, $\dot{x}_0 = -8.985877859$ m/s,

$\dot{y}_0 = -121.605674977$ m/s, $\dot{z}_0 = 9.457952755$ m/s

The above data are measured with respect to the L_2 libration point.

The simulation scenario is assumed such that the formation is initialized at $[x(0)\ \dot{x}(0)\ y(0)\ \dot{y}(0)\ z(0)\ \dot{z}(0)]^T = [0.05\ 0\ 0.05\ 0\ 0.05\ 0]^T$ km. The spacecraft is commanded to keep a constant distance of $\|\boldsymbol{\rho}_c\| = 1\ km$. These numbers were chosen arbitrarily to demonstrate the ability of the proposed controller to provide precise formation flying under such stringent requirements. The reference relative trajectory is chosen to be a constant offset. That is, $x_r = 0.5\sqrt{2}, y_r = 0.5\sqrt{2}, z_r = 0$ for the upper right spacecraft, $x_r = -0.5\sqrt{2}, y_r = 0.5\sqrt{2}, z_r = 0$ for the upper left, $x_r = -0.5\sqrt{2}, y_r = -0.5\sqrt{2}, z_r = 0$ for the lower left and $x_r = 0.5\sqrt{2}, y_r = -0.5\sqrt{2}, z_r = 0$ for the lower right. It is assumed that the mass of the follower spacecraft is 500 kg.

In the $\theta - D$ optimal control design, **Q** and **R** are tuned to give a satisfactory performance. The values of **Q** and **R** are chosen to be

$\mathbf{Q} = diag\{10^{13}, 0, 10^{13}, 0, 10^{12}, 0, 0\}$, $\mathbf{R} = diag\{1,1,1\}$

$\mathbf{D}_1$ and $\mathbf{D}_2$ in (21) and (22) are chosen to be:

$$\mathbf{D}_1 = 0.9e^{-10t}\left[-\frac{\mathbf{T}_0\mathbf{A}(\boldsymbol{x})}{\theta} - \frac{\mathbf{A}^T(\boldsymbol{x})\mathbf{T}_0}{\theta}\right],$$

$$\mathbf{D}_2 = 0.9e^{-10t}\left[-\frac{\mathbf{T}_0\mathbf{A}(\boldsymbol{x})}{\theta} - \frac{\mathbf{A}^T(\boldsymbol{x})\mathbf{T}_0}{\theta} + \mathbf{T}_1\mathbf{g}\mathbf{R}^{-1}\mathbf{g}^T\mathbf{T}_1\right]$$

A systematic way of selecting the parameters in $\mathbf{D}_1$ and $\mathbf{D}_2$ matrices is given in Xin and Balakrishnan, 2004.

Figure 3 and Fig. 4 show the tracking errors for the upper right spacecraft where $(e_x, e_y, e_z) \triangleq (x_r - x_s \quad y_r - y_s \quad z_r - z_s)$ and $e_r \triangleq \sqrt{e_x^2 + e_y^2 + e_z^2}$. In order to present the error transient responses clearly, the error histories in the first day is shown in Fig. 3. As can be seen, the errors drop down very quickly to near zero in one day. The control components are shown in Fig. 4. The formation control starts from a relative high value of 100 mN in order to drive the relative position error to zero. Then the control drops down quickly to the very small level in one day to maintain the relative position requirement. After one day, the errors are brought down to a magnitude below 1 millimeter as shown in Fig. 5. The three formation control force components and the total control history at the steady states are presented in Fig. 6. As shown in Fig. 6, the steady state control level is about 0.3 μN on average.

Figures 7-9 show the steady state errors for the spacecraft in the upper left, lower left and lower right locations respectively. As can be seen, all the formation errors are driven below 1 millimeter. Control responses are similar to those of the upper right spacecraft and are not shown in the paper for lack of space.

6. CONCLUSIONS

High accuracy control of multiple spacecraft formation flying in deep-space was investigated using a relatively new suboptimal nonlinear control method. The nonlinear relative dynamics were formulated in the framework of the circular restricted three-body problem. Four spacecraft forming a square in the rotational frame were investigated using a virtual structure approach. The center of the VS follows a reference Lissajous trajectory about the L_2 libration point. The $\theta - D$ controller was applied to each of the four spacecraft. This approach provides an approximate closed-form suboptimal feedback controller and is consequently easy to implement. Numerical results demonstrated that the proposed method yields excellent formation keeping accuracy, maintaining millimeter-level precision in this study. Further studies will be performed by adding disturbances such as solar radiation pressure and measurement noise.

REFERENCES

Bryson, A. E. and Y. C. Ho (1975). *Applied Optimal Control,* Hemisphere Publishing Co., New York.

Gurfil, P., M. Idan, and N.J. Kasdin(2003), "Adaptive Neural Control of Deep-Space Formation Flying," *Journal of Guidance, Control and Dynamics*, Vol. **26**, pp. 491-501.

Kapila, V., A. Sparks, J. Buffington and Y. Qiguo (2000), "Spacecraft Formation Flying: Dynamics and Control," *Journal of Guidance, Control and Dynamics*, Vol. **23**, pp. 561-564.

Leitner, J., et al. (2001), "Formation Flight in Space: Distributed Spacecraft Systems Develop New GPS Capabilities, *GPS World*.

Querioz, M.S., V. Kapila,, and Q. Yan (2000), "Adaptive Nonlinear Control of Multiple Spacecraft Formation Flying," *Journal of Guidance, Control and Dynamics*, Vol. **23**, pp. 385-390.

Ren, W. and R.W. Beard (2004), "Decentralized Scheme for Spacecraft Formation Flying via the Virtual Structure Approach," *Journal of Guidance, Control and Dynamics*, Vol. **27**, pp. 73-82.

Scharf, D.P., F.Y. Hadaegh and S. R. Ploen (2004), "A Survey of Spacecraft Formation Flying Guidance and Control (Part II): Control," *Proceedings of American Control Conference*, Vol. **3**, pp. 2976-2985.

Xin, M. and S.N. Balakrishnan (2005) "A New Method for Suboptimal Control of A Class of Nonlinear Systems," *Optimal Control Applications and Methods,* Vol. **26**, No.2.

Xin, M. , S.N. Balakrishnan,, D.T. Stansbery and E.J. Ohlmeyer (2004), "Nonlinear Missile Autopilot Design with Theta-D Technique," *Journal of Guidance, Control and Dynamics,* Vol. **27**, pp. 406-417.

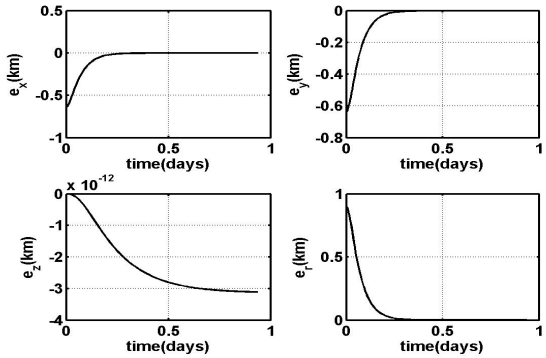

Fig. 3: Upper-right spacecraft formation errors in the 1st day

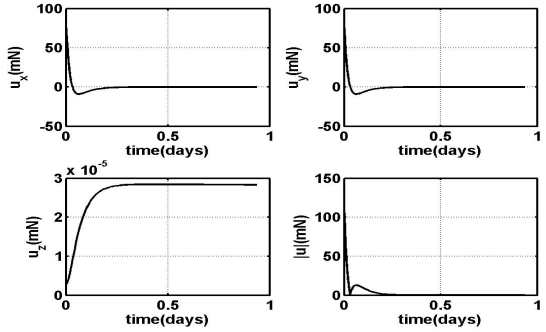

Fig. 4: Upper-right spacecraft formation errors in the 1st day

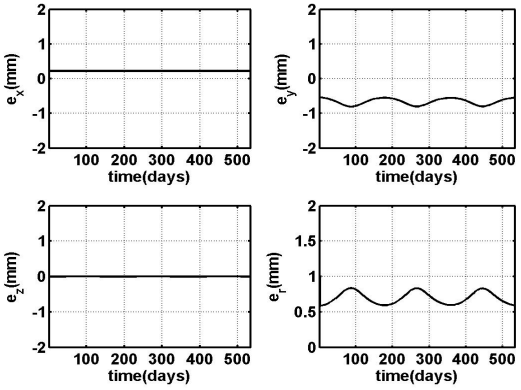

Fig. 5: Upper-right spacecraft steady state errors

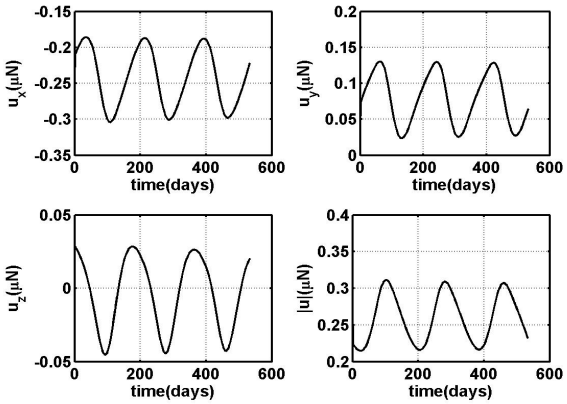

Fig. 6: Upper-right spacecraft steady state control force

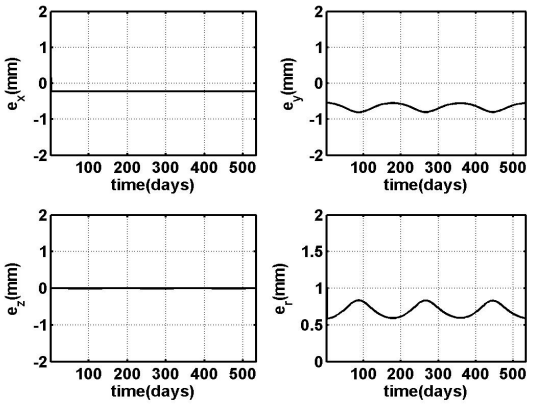

Fig. 7: Upper left spacecraft steady state error

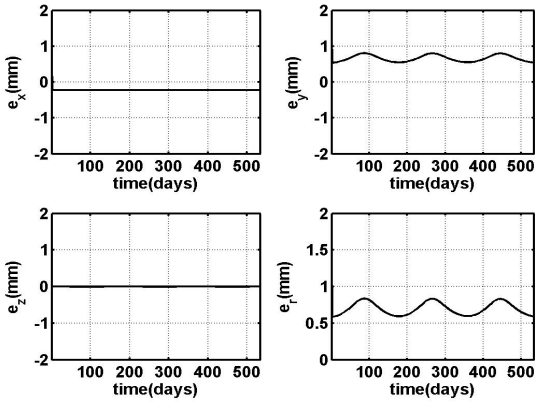

Fig. 8: Lower left spacecraft steady state error

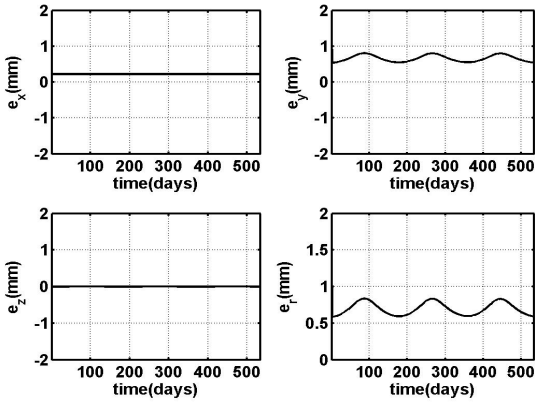

Fig. 9: Lower right spacecraft steady state error